New approach to Data-Driven Variational Multiscale Reduced Order Model (D2-VMS-ROM)

Birgul Koc
birgul.koc@ifpen.fr
birgul.koc@inria.fr

Joint IFPEN – Inria Workshop
5 December 2022, Paris

Education and Work Experience

- **(05/21–05/22) — University of Seville, Seville, Spain**
  - *working with Professor Tomás Chacón on the modeling of the subscales.*

- **(08/16–05/21) — Virginia Tech, Blacksburg, USA, Ph.D. Mathematics**
  - **Advisor:** *Professor Traian Iliescu*
  - **Dissertation:** *Numerical Analysis for Data-Driven Reduced Order Model Closures*

- **(08/16–12/18) — Virginia Tech, Blacksburg, USA, M.S. Mathematics**
  - **Advisor:** *Professor Traian Iliescu*
  - **Thesis:** *Commutation Error in Reduced Order Modeling*

Research Interest

- Applied Mathematics,
- Turbulent Flows,
- Reduced Order Modeling (ROM),
- Closure Modeling,
- Data-Driven Modeling,
- Variational Multiscale Methods,
- Numerical Analysis.

Collaborators

- Guillaume Enchéry, IFPEN
- Angelo Iollo, INRIA & University of Bordeaux
- Tommaso Taddei, INRIA

- Tomás Chacón, University of Seville
- Samuele Rubino, University of Seville

- Traian Iliescu, Virginia Tech
- Honghu Liu, Virginia Tech
- Changhong Mou, University of Wisconsin
- Gianluigi Rozza, SISSA
- Zhu Wang, University of South Carolina
- Omer San, Oklahoma State University
- Leo Rebholz, Clemson University

Outline

- Introduction
- Reduced Order Model (ROM)
- Proper Orthogonal Decomposition (POD)
- Galerkin ROM (G-ROM)
- ROM Closure Problem
- Data-Driven Variational Multiscale ROM (D2-VMS-ROM)
    - Variational Multiscale Framework
    - Data-Driven Approach
        - Coefficient-based D2-VMS-ROM (C-D2-VMS-ROM)
        - Residual-based D2-VMS-ROM (R-D2-VMS-ROM)
- Conclusions

Full Order Models (FOMs), e.g., FE, FV, FD,...

(i) **dimension:** $N = \mathcal{O}(10^6)$ ☹ (e.g., FE mass matrix, $M_h \in R^{N \times N}$)

(ii) **computational cost** ☹

(iii) **accuracy** ☺

Reduced Order Models (ROMs)

(i) **dimension:** $r = \mathcal{O}(10)$ ☺ (e.g., ROM mass matrix, $M_r = C^\top M_h C \in R^{r \times r}$)

(ii) **computational cost** ☺

(iii) **accuracy**

(iiia) **laminar flows:** G-ROM ☺

(iiib) **turbulent flows:** G-ROM ☹ G-ROM + closure term ☺

Reduced Order Model (ROM)

Question: What kind of setting is good for the ROM?

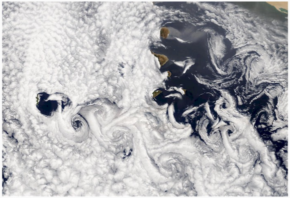

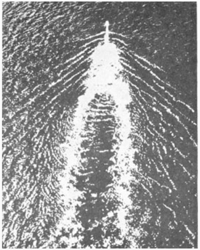

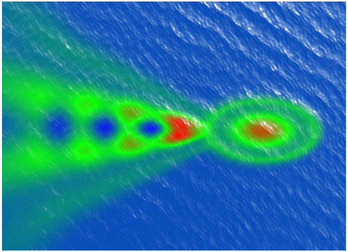

Proper Orthogonal Decomposition (POD)

- one of the most popular ROM techniques,
- seeks a low-dimensional basis $\{\varphi_j\}_{j=1}^{r}$,
  - data for the parabolic PDE:

$$\dot{\boldsymbol{u}} = \boldsymbol{f}(\boldsymbol{u}), \tag{1}$$

  - collect the snapshots $\left\{\boldsymbol{u}_h^1, \dots, \boldsymbol{u}_h^M\right\}$ from FE solutions,
  - solve the minimization problem:

$$\min_{(\varphi_i,\varphi_j)_{\mathcal{H}}=\delta_{ij}} \frac{1}{M} \sum_{j=1}^{M} \left\| \boldsymbol{u}_h(t_j) - \sum_{i=1}^{d} \Big(\boldsymbol{u}_h(t_j), \varphi_i(x)\Big)_{\mathcal{H}} \varphi_i(x) \right\|^2, \tag{2}$$

  - solve the eigenvalue problem:

$$K v_i = \lambda_i v_i \quad , \quad K = \frac{1}{M} Y^T M_h Y \tag{3}$$

$$\lambda_1 \geqslant \lambda_2 \geqslant \dots \lambda_d \geqslant \lambda_{d+1} = \dots = \lambda_M = 0 \tag{4}$$

$$(C_r)_i = \frac{1}{\sqrt{M}} \frac{1}{\sqrt{\lambda_i}} Y v_i \quad , \quad i = 1, \dots, r. \tag{5}$$

Galerkin ROM (G-ROM)

We derive the G-ROM framework on the incompressible Navier-Stokes equations:

$$\frac{\partial \boldsymbol{u}}{\partial t} - Re^{-1}\Delta \boldsymbol{u} + \boldsymbol{u}\cdot\nabla\boldsymbol{u} + \nabla p = \boldsymbol{0}\,, \tag{6}$$

$$\nabla\cdot\boldsymbol{u} = 0\,, \tag{7}$$

- the most straightforward ROM,
- build the ROM solution, i.e., $\boldsymbol{u}_r$ as ($\boldsymbol{u}_d$ is truth solution)

$$\boldsymbol{u}_r = \sum_{i=1}^{r} (\boldsymbol{a}_r)_i\, \varphi_i. \tag{8}$$

- find the weak form of (6)-(7) by inserting $\boldsymbol{u}_r$ into $\boldsymbol{u}$ in (6)-(7)

$$\boxed{\textbf{G-ROM:}\quad \dot{\boldsymbol{a}}_r = A\,\boldsymbol{a}_r + \boldsymbol{a}_r^{\top}\, B\,\boldsymbol{a}_r,} \tag{9}$$

  - $\boldsymbol{a}$ is the unknown,
  - the matrix $A_{im} = -Re^{-1}\,(\nabla\boldsymbol{\varphi}_m, \nabla\boldsymbol{\varphi}_i)$,
  - the tensor $B_{imn} = -\big(\boldsymbol{\varphi}_m\cdot\nabla\boldsymbol{\varphi}_n, \boldsymbol{\varphi}_i\big)\, 1 \le i, m, n \le r\,.$

ROM Closure Problem

Structure-dominated Regime

- the rate is fast,
- resolved regime,
- closure term is not needed, e.g., G-ROM

Convection-dominated Regime

- the rate is not fast,
- under-resolved regime,
- to increase the numerical accuracy
    - $r \uparrow$ ☹
    - add a closure ☺

$$(\dot{\boldsymbol{u}}_r, \varphi_i) = (\boldsymbol{f}(\boldsymbol{u}_r), \varphi_i) + \text{Closure term}. \tag{10}$$

Closure term:

- models the interaction between the resolved and unresolved ROM modes,
- is not a closed term,
- is modeled with r-dimensional operators in an offline stage.

ROM Closure Modeling

Question: How do we model the closure term?

- Functional ROM closures
  - physical insight,
  - e.g., eddy viscosity.
- Structural ROM closures
  - mathematical arguments,
  - e.g., approximate deconvolution, parameterized manifolds, data-driven.

Data-Driven Framework (D2):

- ansatz construction

$$\text{Closure term}(\boldsymbol{a}_d, \boldsymbol{a}_r) \approx \text{Ansatz}(\boldsymbol{a}_r), \tag{11}$$

- least-squares problem

$$\min_{\textbf{D2 operators}} \sum_{j=1}^{M} \left\| \text{Closure term}\left((\boldsymbol{a}_d)_j^{\text{FOM}}, (\boldsymbol{a}_r)_j^{\text{FOM}}\right) - \text{Ansatz}\left((\boldsymbol{a}_r)_j^{\text{FOM}}\right) \right\|^2 \tag{12}$$

$$\boxed{\textbf{D2-VMS-ROM:} \quad (\dot{\boldsymbol{u}}_r, \varphi_i) = (\boldsymbol{f}(\boldsymbol{u}_r), \varphi_i) + \text{Ansatz}(\boldsymbol{a}_r)} \tag{13}$$

Ref: *Mou C., Koc B., San O., Rebholz L.G., and Iliescu T. (2021). Data-driven variational multiscale reduced order models. Computer Methods in Applied Mechanics and Engineering, 373:11347.*

2S-D2-VMS-ROM

- using hierarchical structure of ROM space and basis
- resolved ROM scales $\boldsymbol{X}_1 := \text{span}\{\boldsymbol{\varphi}_1, \ldots, \boldsymbol{\varphi}_r\}$
- unresolved ROM scales $\boldsymbol{X}_2 := \text{span}\{\boldsymbol{\varphi}_{r+1}, \ldots, \boldsymbol{\varphi}_d\}$
- two-scale decomposition
    - $\boldsymbol{u}_r \in \boldsymbol{X}_1$ resolved ROM component of $\boldsymbol{u}$
    - $\boldsymbol{u}' \in \boldsymbol{X}_2$ unresolved ROM component of $\boldsymbol{u}$

$$\boldsymbol{u}_d = \sum_{j=1}^{d} a_j \varphi_j = \sum_{j=1}^{r} (\boldsymbol{a}_r)_j \varphi_j + \sum_{j=r+1}^{d} (\boldsymbol{a}')_j \varphi_j = \boldsymbol{u}_r + \boldsymbol{u}'$$

- VMS-ROM closure term

$$\left(\dot{\boldsymbol{u}}_r, \varphi_i\right) = \left(\boldsymbol{f}(\boldsymbol{u}_r), \varphi_i\right) + \underbrace{\boxed{\left[\left(\boldsymbol{f}(\boldsymbol{u}_d), \varphi_i\right) - \left(\boldsymbol{f}(\boldsymbol{u}_r), \varphi_i\right)\right]}}_{\text{VMS-ROM closure term}} \quad \forall\, i = 1, \ldots, r$$

2S-D2-VMS-ROM Algorithm:

- use the FOM data (snapshots)
- offline stage
- low-dimensional D2 operators
- coefficient-based ansatz:

$$\text{VMS-ROM Closure term} \approx \tilde{\boldsymbol{A}}\boldsymbol{a}_r + \boldsymbol{a}_r^\top \tilde{\boldsymbol{B}}\boldsymbol{a}_r \tag{14}$$

$$\min_{\tilde{\boldsymbol{A}},\tilde{\boldsymbol{B}}} \sum_{j=1}^{M} \left\| \text{Closure term}\Big((\boldsymbol{a}_d)_j^{\text{FOM}}, (\boldsymbol{a}_r)_j^{\text{FOM}}\Big) - \Big[\tilde{\boldsymbol{A}}(\boldsymbol{a}_r^{FOM})_j + ((\boldsymbol{a}_r^{FOM})_j)^\top \tilde{\boldsymbol{B}}(\boldsymbol{a}_r^{FOM})_j\Big] \right\|^2 \tag{15}$$

$$\boxed{\textbf{2S-D2-VMS-ROM:} \quad \dot{\boldsymbol{a}} = (A + \tilde{A})\boldsymbol{a}_r + \boldsymbol{a}_r^\top (B + \tilde{B})\boldsymbol{a}_r} \tag{16}$$

3S-D2-VMS-ROM

- large resolved ROM scales $\boldsymbol{X}_1 := \text{span}\{\varphi_1, \ldots, \varphi_{r_1}\}$
- small resolved ROM scales $\boldsymbol{X}_2 := \text{span}\{\varphi_{r_1+1}, \ldots, \varphi_r\}$
- unresolved ROM scales $\boldsymbol{X}_3 := \text{span}\{\varphi_{r+1}, \ldots, \varphi_d\}$

- **three-scale decomposition:**
  - $\boldsymbol{u}_L \in \boldsymbol{X}_1$ large resolved ROM component of $\boldsymbol{u}$
  - $\boldsymbol{u}_S \in \boldsymbol{X}_2$ small resolved ROM component of $\boldsymbol{u}$
  - $\boldsymbol{u}' \in \boldsymbol{X}_3$ unresolved ROM component of $\boldsymbol{u}$

$$\boldsymbol{u}_d = \sum_{j=1}^{d} a_j \, \varphi_j = \sum_{j=1}^{r_1} (\boldsymbol{a}_L)_j \, \varphi_j + \sum_{j=r_1+1}^{r} (\boldsymbol{a}_S)_j \, \varphi_j \sum_{j=r+1}^{d} (\boldsymbol{a}')_j \, \varphi_j = \boldsymbol{u}_L + \boldsymbol{u}_S + \boldsymbol{u}' = \boldsymbol{u}_r + \boldsymbol{u}'$$

- **VMS-ROM closure terms**
  - large-small VMS-ROM closure term:

$$(\dot{\boldsymbol{u}}_L, \varphi_i) = (\boldsymbol{f}(\boldsymbol{u}_r), \varphi_i) + \left[\left(\boldsymbol{f}(\boldsymbol{u}_d), \varphi_i\right) - (\boldsymbol{f}(\boldsymbol{u}_r), \varphi_i)\right] \quad \forall \, \boldsymbol{i} = \mathbf{1}, \ldots, \boldsymbol{r}_1,$$

  - small-unresolved VMS-ROM closure term:

$$(\dot{\boldsymbol{u}}_S, \varphi_i) = (\boldsymbol{f}(\boldsymbol{u}_r), \varphi_i) + \left[\left(\boldsymbol{f}(\boldsymbol{u}_d), \varphi_i\right) - (\boldsymbol{f}(\boldsymbol{u}_r), \varphi_i)\right] \quad \forall \, \boldsymbol{i} = \boldsymbol{r}_1 + \mathbf{1}, \ldots, \boldsymbol{r},$$

continued

- two different least squares problems:
  - 1st one: large and small resolved scales; produces $\tilde{A}_L$ and $\tilde{B}_L$
  - 2nd one: small resolved and unresolved scales; produces $\tilde{A}_S$ and $\tilde{B}_S$

$$\begin{bmatrix} \dot{\boldsymbol{a}}_L \\ \dot{\boldsymbol{a}}_S \end{bmatrix} = A\,\boldsymbol{a} + \boldsymbol{a}^\top B\,\boldsymbol{a} + \begin{bmatrix} \tilde{A}_L\,\boldsymbol{a}_L + \boldsymbol{a}_L^\top\,\tilde{B}_L\,\boldsymbol{a}_L \\ \tilde{A}_S\,\boldsymbol{a}_S + \boldsymbol{a}_S^\top\,\tilde{B}_S\,\boldsymbol{a}_S \end{bmatrix}, \tag{17}$$

  - 2 truncated SVD
  - more flexibility in choosing the VMS-ROM closure operators $\tilde{A}_L, \tilde{A}_S, \tilde{B}_L$, and $\tilde{B}_S$ in the least squares problems.

Numerical results are obtained by using the Burgers and NSE equations considering the reconstructive and predictive regimes.

$$\begin{cases} u_t - \nu u_{xx} + u u_x = 0 \ , & x \in [0,1], \ t \in [0,1], \\ u(0,t) = u(1,t) = 0 \ , & t \in [0,1], \end{cases} \tag{18}$$

with the initial condition

$$u_0(x) = \begin{cases} 1, & x \in (0, 1/2], \\ 0, & x \in (1/2, 1], \end{cases} \tag{19}$$

Snapshot Generation: $\nu = 10^{-3}, h = 1/2048, \Delta t = 10^{-3}$, linear FE, CN.

r	G-ROM	2S-D2-VMS-ROM	3S-D2-VMS-ROM		
	$\mathcal{E}(L^2)$	$\mathcal{E}(L^2)$	r_1	tol_S	$\mathcal{E}(L^2)$
3	1.181e-01	7.278e-02	1	1e+00	1.322e-02
7	1.828e-01	1.755e-01	2	1e-03	3.915e-03
11	1.258e-01	1.229e-01	1	1e-03	1.787e-03
17	6.551e-02	6.456e-02	1	1e-02	2.310e-03

Table 1: Reconstructive regime, $tol = tol_L = 10^1$, and optimal tol_S.

Predictive regime: training set = [0,0.7] and testing set = [0.7,1].

r	G-ROM	2S-D2-VMS-ROM		3S-D2-VMS-ROM			
	$\mathcal{E}(L^2)$	tol	$\mathcal{E}(L^2)$	r_1	tol_S	tol_L	$\mathcal{E}(L^2)$
3	2.185e-01	1e-01	3.623e-02	2	1e-01	1e+00	3.029e-02
7	2.054e-01	3e-02	2.004e-02	6	5e-02	3e-02	1.428e-02
11	1.620e-01	3e-02	1.608e-02	10	5e-02	3e-02	1.418e-02
17	1.103e-01	1e-02	1.524e-02	6	1e-02	1e-01	1.506e-02

Table 2: Predictive regime, optimal tol, tol_S, and tol_L.

Conclusions:

- 3S-D2-VMS-ROM has more flexibility in choosing the VMS-ROM closure operators.
- 3S-D2-VMS-ROM is significantly more accurate than the 2S-D2-VMS-ROM for reconstructive regime.
- 3S-D2-VMS-ROM is more accurate than the 2S-D2-VMS-ROM for predictive regime.

Flow Past a Cylinder

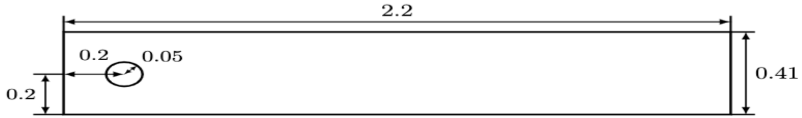

Figure 2: Geometry of the flow past a circular cylinder numerical experiment.

We prescribe no-slip boundary conditions on the walls and cylinder, and the following inflow and outflow profiles:

$$u_1(0, y, t) = u_1(2.2, y, t) = \frac{6}{0.41^2} y(0.41 - y), \tag{20}$$

$$u_2(0, y, t) = u_2(2.2, y, t) = 0, \tag{21}$$

where $\boldsymbol{u} = \langle u_1, u_2 \rangle$.

- DOF: $103K$ (102962) velocity and $76K$ (76725) pressure
- linearized BDF2 temporal discretization with $\Delta t = 0.002$
- $Re = 1000$

ROM Construction:

- use 10s of the FOM data, e.g., $[13, 23]$ (one period=$[13, 13.268]$)
- reconstructive regime: ROM basis=$[13, 23]$, D2 operators=$[13, 13.268]$
- predictive regime: ROM basis=$[13, 23]$, D2 operators=$[13, 13.134]$ (half period)

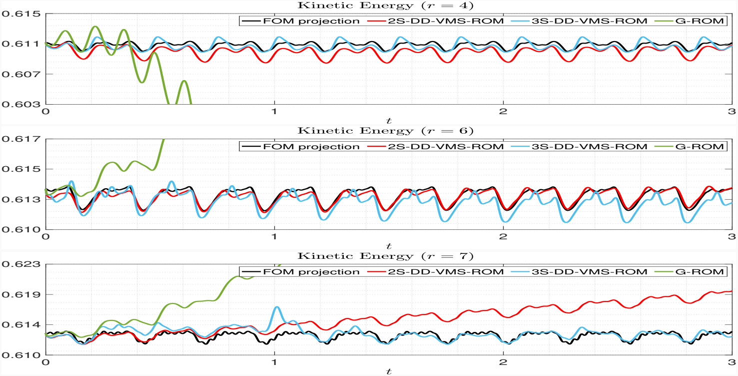

Figure 1: Flow past a cylinder, $Re = 1000$, reconstructive regime. Time evolution of the kinetic energy for G-ROM, 2S-DD-VMS-ROM, and 3S-DD-VMS-ROM for different r values.

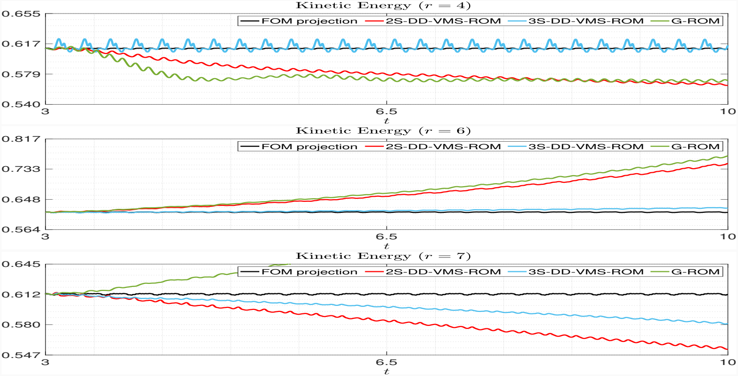

Figure 2: Flow past a cylinder, $Re = 1000$, predictive regime. Time evolution of the kinetic energy for G-ROM, 2S-DD-VMS-ROM, and 3S-DD-VMS-ROM for different r values.

Residual-based Data-Driven Variational Multiscale (R-D2-VMS-ROM)

Ref: *Koc, B., Rebollo, T. C., Iliescu, T. (2022). Residual Data-Driven Variational Multiscale Reduced Order Models for Parameter Dependent Problems. arXiv preprint arXiv:2208.00059.*

Aim: Create a ROM closure model depends on the **ROM residual**

For a given bilinear-linear form:

$$a(\boldsymbol{u}^d, \boldsymbol{v}^d) =< \boldsymbol{f}, \boldsymbol{v}^d > \tag{22}$$

Decompose (22) into two problems as:

$$a(\boldsymbol{u}_L, \boldsymbol{v}_L) + a(\boldsymbol{u}_S, \boldsymbol{v}_L) = \langle \boldsymbol{f}, \boldsymbol{v}_L \rangle \tag{23a}$$

$$a(\boldsymbol{u}_S, \boldsymbol{v}_S) + a(\boldsymbol{u}_L, \boldsymbol{v}_S) = \langle \boldsymbol{f}, \boldsymbol{v}_S \rangle \tag{23b}$$

The matrix-vector form of (23a)-(23b) is as follows:

$$\boldsymbol{A}_{LL}\, \boldsymbol{a}_L + \boldsymbol{A}_{LS}\, \boldsymbol{a}_S = \boldsymbol{b}_L \tag{24a}$$

$$\boldsymbol{A}_{SL}\, \boldsymbol{a}_L + \boldsymbol{A}_{SS}\, \boldsymbol{a}_S = \boldsymbol{b}_S \tag{24b}$$

$$\boxed{\text{Closure}(\boldsymbol{a}_S) \approx \text{Ansatz}(Res(\boldsymbol{a}_L))}.$$

R-D2-VMS-ROM with one ansatz

$$\boldsymbol{a}_S \approx \tilde{\boldsymbol{A}}\, Res_{\boldsymbol{S}}(\boldsymbol{a}_L), \tag{25}$$

where $Res_{\boldsymbol{S}}(\boldsymbol{a}_L) = \boldsymbol{b}_S - \boldsymbol{A}_{SL}\, \boldsymbol{a}_L$.

To construct the D2 operator in (25), we need to solve the following generalized minimization problem:

$$\min_{\tilde{\boldsymbol{A}}} \quad \sum_{j=1}^{M} \left\| \boldsymbol{a}_S^j - \tilde{\boldsymbol{A}}\, Res_{\boldsymbol{S}}(\boldsymbol{a}_L^j) \right\|_{L^2}^2 . \tag{26}$$

$$\boxed{\textbf{R1-ROM}: \left(\boldsymbol{A}_{LL} - \boldsymbol{A}_{LS}\, \tilde{\boldsymbol{A}}\, \boldsymbol{A}_{SL}\right) \boldsymbol{a}_L = \boldsymbol{b}_L - \boldsymbol{A}_{LS}\, \tilde{\boldsymbol{A}}\, \boldsymbol{b}_S.} \tag{27}$$

R-D2-VMS-ROM with two ansatzes

$$\boldsymbol{a}_S \approx \tilde{\boldsymbol{A}}_1 \, Res_{\boldsymbol{S}}(\boldsymbol{a}_L), \tag{28}$$

$$Res_{\boldsymbol{L}}(\boldsymbol{a}_S) \approx \tilde{\boldsymbol{A}}_2 \, Res_{\boldsymbol{L}}(\boldsymbol{a}_S^{approx}), \tag{29}$$

where $Res_{\boldsymbol{L}}(\boldsymbol{a}_S) = \boldsymbol{b}_L - \boldsymbol{A}_{LS} \, \boldsymbol{a}_S$.

By using (26) and the following minimization problems to obtain the D2 operators $\tilde{\boldsymbol{A}}_1$ and $\tilde{\boldsymbol{A}}_2$, respectively.

$$\min_{\tilde{\boldsymbol{A}}_2} \quad \sum_{j=1}^{M} \left\| Res_{\boldsymbol{L}}(\boldsymbol{u}_S^j) - \tilde{\boldsymbol{A}}_2 \, Res_{\boldsymbol{L}}(\boldsymbol{a}_S^{approx}) \right\|_{L^2}^2 . \tag{30}$$

$$\boxed{\textbf{R2-ROM}: \left(\boldsymbol{A}_{LL} - \tilde{\boldsymbol{A}}_2 \, \boldsymbol{A}_{LS} \, \tilde{\boldsymbol{A}}_1 \, \boldsymbol{A}_{SL}\right) \boldsymbol{a}_L = \tilde{\boldsymbol{A}}_2 \left(\boldsymbol{b}_L - \boldsymbol{A}_{LS} \, \tilde{\boldsymbol{A}}_1 \, \boldsymbol{b}_S\right).} \tag{31}$$

Numerical Results

We present numerical results for the parameter-dependent CD problem

$$\begin{cases} -\mu \partial_{xx} u + c \partial_x u = f \quad \text{for } x \in [0,1], \\ u(0) = 0 \quad \text{and} \quad u(1) = 0, \end{cases} \tag{32}$$

with the following exact solution

$$u(x,\mu) = \frac{\exp(cx/\mu) - 1}{\exp(c/\mu) - 1} - x, \tag{33}$$

where μ is a parameter. The force term is $f = -c = -400$.

Snapshot Generation $\mu \in [1, 10]$, $\Delta\mu = 1$, linear FE, $h = 1/4096$.

ROM Construction Use $\mu^{training} = 1, 2, \ldots, 9, 10$ to generate the ROM basis functions and operators and train the D2-VMS-ROM operators. We test all the ROMs for $\mu^{testing} = 0.5, 0.1, 0.05, 15$, which fall outside the training range.

To compare the numerical accuracy of the methods, we use the following metric to compute the ROM errors:

$$\mathcal{E}2_{L^2} = \left\| \boldsymbol{u}_L(\mu^{testing}) - \sum_{i=1}^{L} \left(\boldsymbol{u}^{\text{FOM}}(\mu^{testing}), \boldsymbol{\varphi}_i \right)_{L^2} \boldsymbol{\varphi}_i \right\|_{L^2}. \tag{34}$$

For a fair comparison, we also consider the coefficient-based D2-VMS-ROM:

$$\boldsymbol{A}_{LS}\, \boldsymbol{a}_S \approx \tilde{\boldsymbol{A}}\, \boldsymbol{a}_L, \tag{35a}$$

$$\boxed{\textbf{C-ROM}: \left(\boldsymbol{A}_{LL} + \tilde{\boldsymbol{A}}\right) \boldsymbol{a}_L = \boldsymbol{b}_L.} \tag{36}$$

Testing the ROMs for $\mu = 0.5$

L	G	C	R1	R2
1	4.38e+00	5.72e+00	5.45e-04	3.04e-04
2	3.71e-01	3.66e-01	1.04e-04	8.88e-03
3	4.26e-01	4.19e-01	7.64e-05	3.14e-03
4	1.68e-01	1.68e-01	8.19e-05	1.78e-03
5	1.61e-01	1.61e-01	2.46e-04	1.22e-03
6	9.92e-02	9.92e-02	1.72e-04	8.84e-04
7	9.48e-02	9.48e-02	1.18e-04	6.80e-04

Table 3: L^2 error (34) for G-ROM, C-ROM, R1-ROM, and R2-ROM for various L values.

L	$\boldsymbol{A}_{LS}\,\boldsymbol{a}_S$	C	L	$\boldsymbol{A}_{LS}\,\boldsymbol{a}_S$	C
1	3.06e+02	7.10e+02	6	5.90e+02	2.40e-02
2	1.21e+03	1.77e+01	7	4.18e+02	9.31e-05
3	1.21e+03	1.90e+01	8	2.64e+02	7.84e-05
4	1.00e+03	7.06e-01	9	1.26e+02	1.02e-02
5	7.85e+02	3.76e-01	10	0	0

Table 4: Consistency error comparison for C-D2-VMS-ROM with various L values.

In Tables 4, 5, and 6, to investigate the ROM consistency, we list the norm of the closure term and its ansatz.

L	$\boldsymbol{a}_S$	R1	L	$\boldsymbol{a}_S$	R1
1	6.37e-02	7.01e-02	6	2.95e-03	6.03e-03
2	2.48e-02	2.67e-02	7	2.13e-03	5.12e-03
3	1.14e-02	1.28e-02	8	1.50e-03	7.41e-04
4	6.36e-03	8.77e-03	9	9.35e-04	4.23e-04
5	4.17e-03	7.11e-03	10	0	0

Table 5: Consistency error comparison for R1-D2-VMS-ROM with various L values.

L	$Res_L(\boldsymbol{a}_S)$	R2	L	$Res_L(\boldsymbol{a}_S)$	R2
1	4.24e+01	4.07e+01	6	6.86e+02	9.31e+02
2	1.24e+03	1.32e+03	7	5.31e+02	8.24e+02
3	1.21e+03	1.23e+03	8	4.43e+02	6.97e+03
4	1.06e+03	1.16e+03	9	3.74e+02	3.57e+02
5	8.34e+02	1.00e+03	10	0	0

Table 6: Consistency error comparison for R2-D2-VMS-ROM with various L values.

Testing for All μ Values

Instead of further investigating different $\mu^{testing}$ values that are out of the training set, we use the average L^2 error (37) to measure the ROM consistency for $\mu^{testing} = 0.5, 0.1, 0.05, 15$.

$$\mathcal{E}_{avg} = \frac{1}{M} \sum_{j=1}^{M} \left\| \boldsymbol{u}_L(\mu_j^{testing}) - \sum_{i=1}^{r} \left(\boldsymbol{u}^{\text{FOM}}(\mu_j^{testing}), \boldsymbol{\varphi}_i \right)_{L^2} \boldsymbol{\varphi}_i \right\|_{L^2}. \tag{37}$$

L	G-ROM	C-ROM	R1-ROM	R2-ROM
1	1.95e+01	3.99e-03	8.98e-04	1.14e-03
2	4.17e-01	5.76e-03	2.11e-04	1.13e-02
3	3.31e+00	5.06e-03	2.92e-04	6.24e-03
4	3.07e-01	4.68e-03	3.36e-04	5.36e-03
5	1.93e+00	4.43e-03	1.03e-03	4.91e-03
6	2.64e-01	4.17e-03	8.30e-04	4.53e-03
7	1.49e+00	3.95e-03	6.54e-04	4.25e-03

Table 7: Average L^2 error (37) for G-ROM, C-ROM, R1-ROM, and R2-ROM for various L values.

Conclusions

- The errors in Table 3, the G-ROM and C1-ROM yield the worst results among all the ROMs.
- Furthermore, R1-ROM give the lowest errors among all the ROMs.

- The order of magnitude of the C-ROM error quickly diminishes than the norm of the closure term.
- In Tables 5-6, we observe that the order of magnitude of the R1-ROM and R2-ROM are the same as their closure terms, and as L goes to d. Thus, we conclude that R1-ROM and R2-ROM are equally consistent models.

- Based on the errors in Table 7, G-ROM and R1-ROM are the worst and most accurate, respectively.
- Although R2-ROM involves more information from the sub-scale equation, R1-ROM is more accurate than R2-ROM.